The alpine Swiss-French airborne gravity survey

Originally published in:
Geophysical Journal International 152(1), https://doi.org/10.1046/j.1365-246X.2003.01748.x

Geophys. J. Int. (2003) **152,** 8–19

The alpine Swiss-French airborne gravity survey

Jérôme Verdun,[1,2] Emile E. Klingelé,[1] Roger Bayer,[2]
Marc Cocard,[1] Alain Geiger[1] and Hans-Gert Kahle[1]

[1] *Geodesy and Geodynamic Laboratory, ETH Hönggerberg HPV* G58-2 CH-8093 *Zürich, Switzerland. E-mail: jerome@geod.baug.ethz.ch*
[2] *Laboratoire de Géophysique-Tectonique-Sédimentologie, UMR CNRS* 5573, *Université Montpellier* II, CC060, 34095 *Montpellier Cedex* 5, *France. E-mail: roger@dstu.univ-montp2.fr*

Accepted 2002 April 10. Received 2002 April 10; in original form 2001 July 11

SUMMARY

In February 1998, a regional-scale, airborne gravity survey was carried out over the French Occidental Alps within the framework of the GéoFrance 3-D research program.The survey consisted of 18 NS and 16 EW oriented lines with a spacing of 10 and 20 km respectively, covering the whole of the Western French Alps (total area: 50 000 km^2; total distance of lines flown: 10 000 km). The equipment was mounted in a medium-size aircraft (DeHavilland Twin Otter) flowing at a constant altitude of 5100 m a.s.l, and at a mean ground speed of about 280 km h^{-1}.

Gravity was measured using a LaCoste & Romberg relative, air/sea gravimeter (type SA) mounted on a laser gyro stabilized platform. Data from 5 GPS antennae located on fuselage and wings and 7 ground-based GPS reference stations were used to determine position and aircraft induced accelerations.The gravimeter passband was derived by comparing the vertical accelerations provided by the gravimeter with those estimated from the GPS positions. This comparison showed that the gravimeter is not sensitive to very short wavelength aircraft accelerations, and therefore a simplified formulation for computing airborne gravity measurements was developed. The intermediate and short wavelength, non-gravitational accelerations were eliminated by means of digital, exponential low-pass filters (cut-off wavelength: 16 km).

An important issue in airborne gravimetry is the reliability of the airborne gravity surveys when compared to ground surveys. In our studied area, the differences between the airborne-acquired Bouguer anomaly and the ground upward-continued Bouguer anomaly of the Alps shows a good agreement: the rms of these differences is equal to 7.68 mGal for a spatial resolution of 8 km. However, in some areas with rugged topography, the amplitudes of those differences have a striking correlation with the topography. We then argue that the choice of an appropriate density (reduction by a factor of 10 per cent) for computing the ground topographic corrections over the highest mountains, results in significantly reducing the differences between airborne and ground upward-continued Bouguer anomalies, which shows that some of the misfit stems from errors in the ground data.

Key words: airborne gravimetry, equalization, filtering, upward continuation.

1 INTRODUCTION

With the development of kinematic GPS in the late 1980s, airborne gravimetry has gained an increasing importance, and has proved to be particularly well-suited for the determination of the gravity field of wavelengths ranging from *5* to 100 km, thus filling the gap between ground-based and spaceborne gravity measurement techniques (Balmino *et al.* 1996). Land surveys in mountainous regions are both costly and time consuming. Measurements are strongly influenced by local density anomalies located below and above the measurement stations, and involve the use of time-consuming algorithms during data reduction. Obtaining all measurements on a horizontal surface located above the topography overcomes all the problems above and in addition supplies data which can be easily interpreted using potential field transformation methods. In spite of recent improvements, the wavelengths of spaceborne gravity data are still too long for regional geological investigations. For instance, an area size of the French Alps would be covered by fifty values or less.

Since the first attempt at airborne gravimetry by Thompson and LaCoste in 1958 (Thompson & LaCoste 1960) accuracy and resolution have dramatically increased (Brozena & Peters 1988; Brozena

et al. 1992; Bell *et al.* 1992; Brozena 1994; Gumert 1995; Olesen & Forsberg 1995; Childers *et al.* 1999), although a lack of ground data means that a true determination of the repeatability of these surveys is difficult. In 1992, the Geodesy and Geodynamics Lab of the Swiss Federal Institute of Technology carried out a high-altitude survey (5100 m above sea level) covering the entire territory of Switzerland (Klingelé *et al.* 1997). This survey showed that airborne gravity field measurements can be successfully acquired over areas with very different topographic features (high mountains and deep valleys.

In 1996 the French Ministries of Industry, Research and Public Education initiated an ambitious research programme to investigate the deep structure of France (GéoFrance 3-D). Within the framework of this programme, an airborne gravity survey covering the whole of the French Occidental Alps was planned by the 'Laboratoire de Géophysique-Tectonique-Sédimentologie' (University of Montpellier) in collaboration with the Geodesy and Geodynamics Lab (ETH Zürich). This paper describes all the stages of this experiment, from the gravity data acquisition to the computation of airborne Bouguer gravity anomalies, and finally discusses their precision and resolution by comparing airborne gravity anomaly map to the land survey gravity anomaly map upward continued to the same altitude.

2 THE SURVEY

The survey (Fig. 1a) was acquired at a constant altitude of 5100 m above sea level (a.s.l.) with the measurement lines oriented N–S and E–W. The line spacing was 10 km for the N–S lines and 20 km for the E–W lines. A total of 10 000 line km of data was acquired. The mean ground speed of the aircraft was around 280 km h^{-1}.

The survey was performed using a medium-size, unpressurized cabin aircraft, a DeHavilland Twin Otter, owned by the Swiss Federal Office of Topography, Ministry of Defense, and operated by pilots of the 'Bundesamt für Militärflugplätze'. The same aircraft had already been used during the airborne survey of Switzerland (Klingelé *et al.* 1997). The aircraft is equipped with an automatic pilot, *Collins type AP 106* and with a GPS/LORAN receiver *Trimble 2000* for navigation purposes using differential GPS.

2.1 The gravimeter and stabilized platform

The LaCoste and Romberg Model SA marine gravity meter was used during the survey. Details of the marine gravity meter and stabilized platform have been described previously by LaCoste (1967), LaCoste *et al.* (1982), Bell *et al.* (1991), Brozena & Peters (1988), Brozena (1984), and the model used for this survey by Klingelé *et al.* (1997). This instrument was upgraded for this survey by replacing the mechanical gyroscopes with optical fiber gyroscopes (Post 1967; Halliday 1997). The 1s sampling rate of gravity data gave a mean distance of about 80 m between two successive gravity measurements.

Throughout the survey, static gravity measurements were performed daily at the airport before and after each survey flight. The recording gravimeter readings allowed the instrumental drift rate to be monitored, and thus gravity data was corrected for this effect. At the beginning of a flight line, data contamination can occur when data recording starts before the gravimeter has had sufficient time to equilibrate after a turn. In order to avoid such contamination, a table of expected gravity values was computed for grid of points covering the survey area, with heading and aircraft speed as variables. The operator adjusted the spring tension to the expected value for

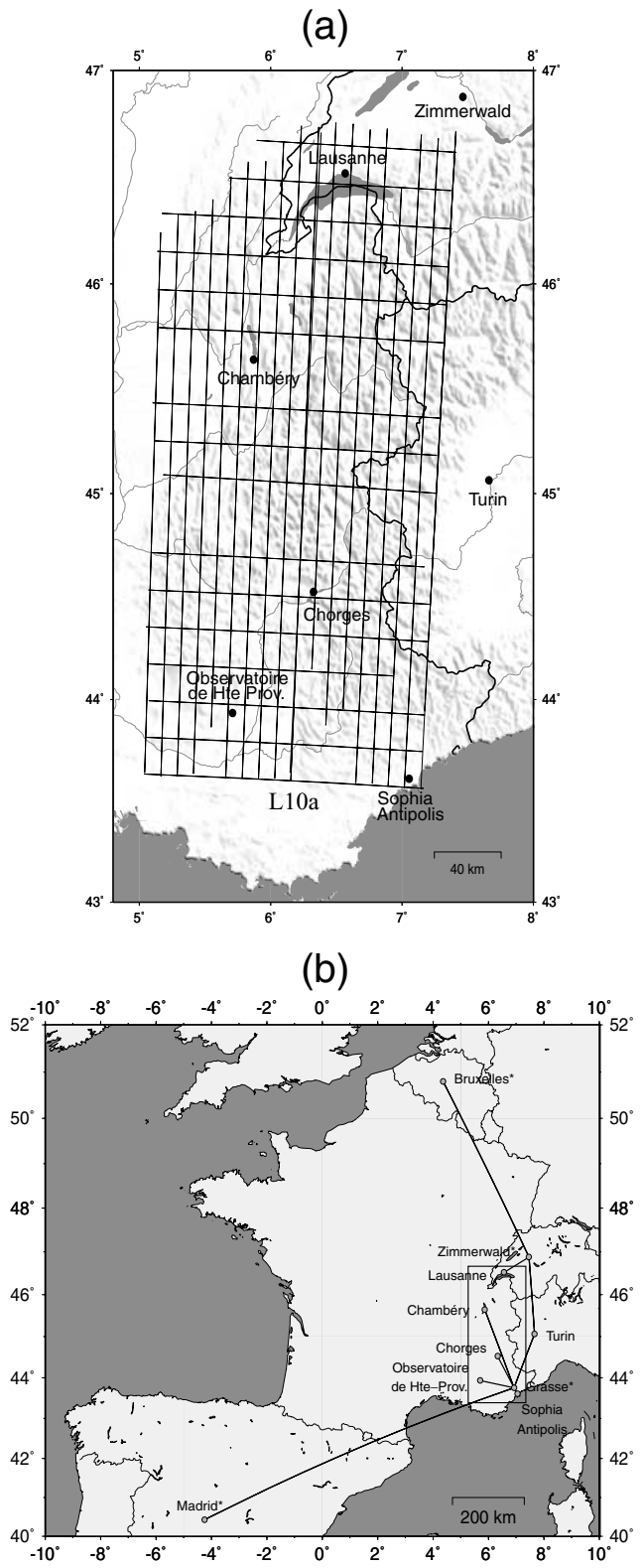

Figure 1. (a) Map showing the N–S and E–W oriented lines flown for the survey at a constant altitude of 5100 m a.s.l.. The line spacing was 10 km for the N–S lines and 20 km for the E–W lines. The sites shown correspond to the seven ground-based GPS stations used for positioning the aircraft during the survey. (b) Location of the GPS stations used for determining the ground-based reference network. The lines joining the GPS stations correspond to the different baselines used to adjust the network. The black box shows the location of the survey area.

the starting point on the next line. Once the aircraft was online and level, the operator unclamped the gravimeter and began recording. Insuring a distance of at least 20 km between the starting point and the first actual point of the survey line allowed the gravimeter platform to stabilize itself before each profile. After each line, once the operator clamped the gravimeter, the pilot began the turn towards the next line.

2.2 GPS receivers

Apart from the GPS/LORAN receiver used for navigation, the aircraft was equipped with five GPS receivers and one high precision inertial system delivering angular velocities and tri-axial accelerations. Two GPS antennae were mounted on the cabin roof, two others on the covers of both engines, and the last one on the top of the tail, thus providing an aircraft reference frame. The use of such a configuration allowed us to ensure redundancy in the determination of the pitch, roll and yaw angles. Seven GPS ground stations operated at a sampling rate of 1 s in order to provide the necessary terrestrial reference frame (Fig. 1a).

All inertial and time-dependent disturbing accelerations have to be separated from the time-independent gravity. In order to do this special filtering techniques and algorithms have been developed. The inertial package operates at a sampling rate ranging from 50 to 100 Hz. It provides information on short-term accelerations, which remain undetected by GPS operating at a 1 to 4 Hz sampling rate.

3 DATA PROCESSING

3.1 Ground-based reference frame

The first step was to combine GPS data obtained from the six ground-based GPS stations with the data provided by four reference stations (Bruxelles, Madrid, Grasse, Zimmerwald) of the IGS international geodetic network, in order to calculate the daily positions of a ten station, terrestrial geodetic network formed by nine baselines (Fig. 1b). By using the Bernese software, version 4.0 (Rothacher & Mervart 1996), the unknown geocentric coordinates were determined with a statistical accuracy in the order of 2 mm, giving a reliable terrestrial reference frame to study the aircraft trajectory.

3.2 Aircraft coordinates and motion-induced accelerations

The development of the technique of processing multi-antenna GPS measurements took advantage of the software developed by ETH for its airborne relative gravity project (1991–1995) (Cocard 1995). In order to obtain the gravity, g, the total vertical acceleration measured on board, g_{airborne}, has to be corrected for the vertical acceleration, a_v, of the gravimeter centre of mass and the Eötvös acceleration, $a_{\text{Eöt}}$. The two corrections are calculated from GPS derived measurements of the altitude, latitude, azimuth, and horizontal velocity of the aircraft (Harlan 1968). So, the actual gravity, g, is given by

$$g = g_{\text{airborne}} - a_v - a_{\text{Eöt}}. \tag{3.1}$$

The ellipsoidal heights of the aircraft derived from GPS processing were transformed into normal heights by using a geoid grid of the French territory computed by Duquenne (1997). The absolute GPS-determined aircraft positions are accurate to within 0.5 m for the horizontal components, and 1 m for the altitude. These error values were determined by calculating the standard deviation of the aircraft positions provided by the different GPS antennae, and reduced to the gravimeter centre of mass. Because over the survey area, observable gravity-field wavelengths at an altitude of 5100 m a.s.l. cannot actually be smaller than 5 km (Fig. 2), an accuracy of 0.5 m is sufficient for the horizontal positioning. Moreover, by supposing a vertical gravity gradient equal to 0.3 mGal m^{-1} (upper limit), then an error of 1 m in the altitude will cause a maximum error of 0.3 mGal in the measured free-air gravity field.

Averaging the various determinations of the Eötvös and vertical accelerations gives the mean value of these quantities at each point along flightline. Then, the error on these correcting accelerations can be estimated by calculating the standard deviation of the differences between the actual values and the mean values along all the lines. By doing so, the Eötvös acceleration accuracy has been estimated to be within 0.3 mGal. However, vertical aircraft accelerations exhibit erratic fluctuations which complicate estimates of their accuracy. As we discuss below, because the survey was performed at a high altitude above the gravity sources, the amplitudes of the observable gravity field wavelengths are significantly greater than those of vertical aircraft acceleration. If gravity meter system will naturally attenuate such high frequency, disturbing accelerations, then correcting gravimeter measurements for their effects is irrelevant for gravity surveys carried out at a high altitude above the sources.

3.3 Gravimeter's measurements

In dynamic mode, the general differential equation driving the motion of the beam is given by (LaCoste 1967)

$$\frac{d^2B}{dt^2} + 2\mu\omega_0\frac{dB}{dt} + {\omega_0}^2(1 - \varepsilon a_h)B = \mathcal{G}S$$
$$- g_{\text{airborne}} = \mathcal{G}S - (g + a_v + a_{\text{Eöt}}), \tag{3.2}$$

where,

B represents the beam position and the related quantities $\frac{dB}{dt}$ and $\frac{d^2B}{dt^2}$ are the beam velocity and acceleration respectively,

$\mathcal{G}S$ is the spring tension i.e. the vertical force per unit mass exerted by the spring,

a_h is the horizontal aircraft acceleration along the direction of flight,

ω_0, μ correspond respectively to the natural angular frequency and the damping factor of the gravimeter system,

ε is a geometrical coefficient which depends on the gravimeter design.

This equation states as long as the axis of the gravity sensor is aligned with the local vertical. The stabilized platform that supports the gravimeter is devoted to maintaining this alignment. The beam position and the spring tension are recorded digitally by the gravimeter system every second.

Our recent work (Verdun *et al.* 2002) suggests that in the survey, the resolvable gravity field wavelengths are higher than those induced by aircraft motion. As a result, variations in the gravity field presumably give rise to long period beam movements when compared to these caused by aircraft accelerations. In order to allow for this effect, it is useful to divide the beam position into two constituents as follows

$$B = \bar{B} + \tilde{B} \tag{3.3}$$

where,

$\bar{B}$ is the average value of the beam position B over a given time interval T,

(a)

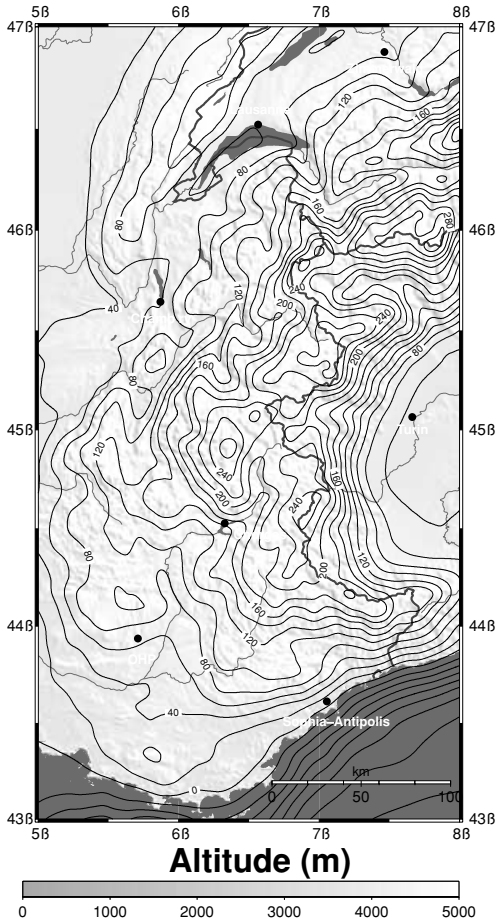

(b)

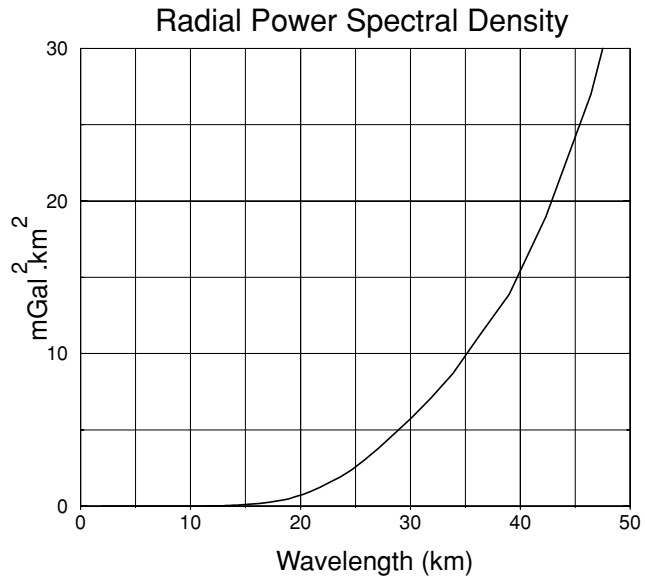

Figure 2. Map showing the gravitational effect of the topography computed at 5100 m a.s.l. using a DEM of the region (a), and the corresponding radial power spectral density (b) as a function of the wavelength. Clearly, observable gravity field wavelengths at 5100 m a.s.l. cannot be smaller than 5 km.

$\tilde{B}$ is its fluctuating constituent over the same time interval.

The value of T must be chosen so that variations in the gravity field remain nearly constant during time intervals of length T. By so doing, the average value $\bar{B}$ cannot contain constituents of periods smaller than those of the gravity field constituents. In other words, the average value $\bar{B}$ can be extracted from the beam position by low-pass filtering using a cut-off frequency greater or equal to the highest frequency of variations in the gravity field. The same procedure can be also applied to the other terms of eq. (3.2) which vary with time. Then, by substituting (3.3) into eq. (3.2) and by separating out average values from fluctuating terms, one obtains the differential equation driving the long period movement of the beam

$$\frac{d^2\bar{B}}{dt^2} + 2\mu\omega_0\frac{d\bar{B}}{dt} + \omega_0^2(1 - \varepsilon\bar{a}_h)\bar{B} = \mathcal{G}\bar{S} - \bar{g} - \bar{a}_v - \bar{a}_{\text{Eöt}}. \tag{3.4}$$

According to our definition of average value, it is clear that the average value of the gravity equals the gravity itself, thus giving

$$\bar{g} = g. \tag{3.5}$$

Moreover, studies of the power spectrum densities of aircraft accelerations for this survey indicate that the average values of the horizontal and vertical aircraft accelerations are negligible quantities (Verdun *et al.* 2002). Eq. (3.4) can therefore by simplified as follows

$$\frac{d^2\bar{B}}{dt^2} + 2\mu\omega_0\frac{d\bar{B}}{dt} + \omega_0^2\bar{B} = \mathcal{G}\bar{S} - g - \bar{a}_{\text{Eöt}}. \tag{3.6}$$

The resulting differential equation corresponds to the response of a damped oscillator excited by the difference between the spring tension and the sum of gravity and Eötvös acceleration. The oscillator passband was calculated from experimentally determined estimates of the damping factor, μ, and the natural frequency, ω_0 (Verdun *et al.* 2002). Then we showed using spectral analysis that the frequencies of the harmonic constituents of gravity, average spring tension, and Eötvös acceleration lie out of the oscillator passband and thus, cannot significantly excite the average movement of the beam. As a result, the first term of (3.6) remains essentially equal to 0. A simplified formulation can be proposed for the processing of gravity data acquired at high altitude using the following equation

$$g = \mathcal{G}\bar{S} - \bar{a}_{\text{Eöt}}, \tag{3.7}$$

where $\mathcal{G}\bar{S}$ and $\bar{a}_{\text{Eöt}}$ represent the spring tension and the Eötvös acceleration, respectively, corrected for high frequency effects by means of low-pass filtering.

3.4 Filtering procedures

Low-pass filtering is intended to remove high frequency, disturbing fluctuations that affect both the spring tension and the Eötvös acceleration. With an eye to easily estimating the filter passband, we designed a so-called exponential low-pass filter whose frequency response is given by

$$\mathcal{H}(f) = \exp(-af), \tag{3.8}$$

where f is the reduced frequency, and a is a dimensionless parameter which is related to the minimum wavelength, $\lambda_{\min}$, of the filter passband (Verdun *et al.* 2002). By setting $\lambda_{\min}$ to 16 km, a satisfactory signal-to-noise ratio was achieved (Fig. 3). It should be noticed that the use of such a filter is equivalent to upward continuing the gravity

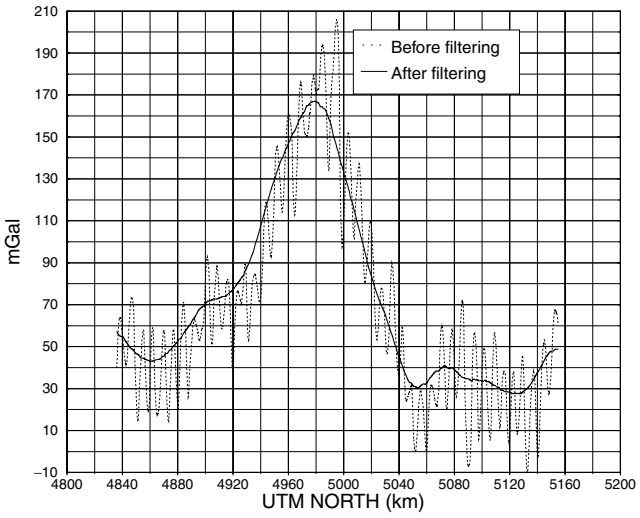

Figure 3. Example of free-air anomaly recorded along flightline L10a, highlighted in Fig. 1(a), as a function of UTM North coordinate. Free-air anomaly is plotted before filtering (dotted line) and after exponential filtering (solid line) with a cut-off wavelength $\lambda_{\min} = 16$ km. The filtered anomaly does not contain spectral constituents of wavelength lower than 16 km.

data to a height 7.6 km above the plane of observation (Blakely 1996). This kind of filter takes advantage of the natural exponential decay of the gravity field spectral constituents with height of measurement, and thereby exponential filtering has a physical sensible interpretation. Moreover, the transient of the filter is rather short causing only a few lost of data at the beginning of flightlines.

3.5 Adjustment of the survey

Airborne gravity surveys invariably exhibit discrepancies at intersections of surveys lines, which have to be removed before any meaningful contour map can be performed. The misties are caused by many effects such as inaccuracies in the GPS solutions and errors introduced from an off-level platform (Bell *et al.* 1999). Moreover, when performing high altitude airborne gravity surveys using an aircraft with non-pressurized cabin, the gravity meter is subjected to significant pressure variations from the airport to the survey area. As matters stand, we do not exactly know to what extent the pressurized chamber of the LaCoste and Romberg gravimeter can withstand such pressure variations. Presumably, the resulting perturbations affecting the gravity sensor might cause substantial offsets in the gravity measurements.

Once a complete set of gravity profiles had been reduced, we calculated the misties at profile intersections using Wessel (1989)'s procedure. Sections of profiles with large misties were removed. In order to adjust the survey lines, we used a method based upon quality weighting assignments using a variance criterion, and which theory is rigorously developed in Mittal (1984). The method uses the normalized sum of squares of misties with other lines as the criterion for assigning a quality weighting to any line. Displaying these weightings allowed us to remove the profiles exhibiting poor quality gravity data in comparison to good profiles, and indicated by very weak quality weightings. The method also provides the dc shifts that have to be applied to each crossover value to reduce the misties to zero. Once the crossover values have been corrected, the other gravity data along the profiles between the intersections can be adjusted by simply distributing the dc corrections in a linear manner.

Before adjustment and line selection, the initial standard deviation of crossover errors was rather high (15.34 mGal) due to the presence of both outliers and data sections of poor quality data. Among the initial 36 airborne gravity profiles, we selected 13 N–S lines and 13 E–W lines which intersect at 126 crossovers. After adjustment, the overall crossover errors achieved a standard deviation of 0.012 mGal, thus engendering confidence in the quality of the data acquired along the selected lines.

3.6 Airborne Bouguer gravity anomaly map

The airborne Bouguer gravity anomaly $\mathcal{B}g$ at any point M is given by

$$\mathcal{B}g(M) = g(M) - \gamma_h(Q) - \mathcal{E}_{\text{topo}}(M),$$

where,

$g(M)$ is the airborne-acquired gravity after filtering and equalization,

$\gamma_h(Q)$ is the normal gravity calculated at the point Q located on the vertical passing through the point M at an altitude equal to the ellipsoidal altitude h of the point M,

$\varepsilon_{\text{topo}}(M)$ is the gravitational effect of the topography, previously filtered with the same procedure as $g(M)$.

The normal gravity was computed by means of Somigliana's closed formula related to the Geodetic Reference System 1980 (GRS80), and corrected for the effect of altitude by using a second order approximation (Moritz 1988). The topographic corrections of airborne gravity data were calculated out to a radius of 167 km with a density of 2670 kg m^{-3}. The gravitational effect of the topography was calculated at each point by adding the contributions of vertical prisms with a surface area of 1 km^2, and a height equal to the topography provided by a digital terrain model of the Alps. This digital elevation model was extracted from the 30-arcsec database GTOPO30 (US Geological Survey's EROS Data Center, Sioux Falls, South Dakota, USA). A resolution of about 1 km proved to be sufficient for the computation of the topographic corrections with an accuracy better than 0.5 mGal (Klingelé *et al.* 1996). The airborne Bouguer gravity anomaly map computed with a resolution of 8 km (half of the cut-off wavelength $\lambda_{\min}$), is shown in Fig. 4.

4 COMPARISON OF AIRBORNE AND GROUND BOUGUER GRAVITY ANOMALIES

In order to assess the reliability of the airborne measurements, the airborne Bouguer gravity anomaly has been compared to the alpine surface Bouguer gravity anomaly upward continued to the same altitude. The purposes of this section are to outline the various stages needed to perform this comparison, and to highlight the difficulty of directly comparing airborne acquired data and ground gravity data in areas of rugged topography.

4.1 The database of the 'Bureau Gravimétrique International'

The land gravity measurements used to produce surface gravity anomaly maps were obtained from the database of the 'Bureau Gravimétrique International', and completed by gravity data acquired during recent surveys over the Alps obtained as part of GéoFrance 3-D research program (Masson *et al.* 1999). Because

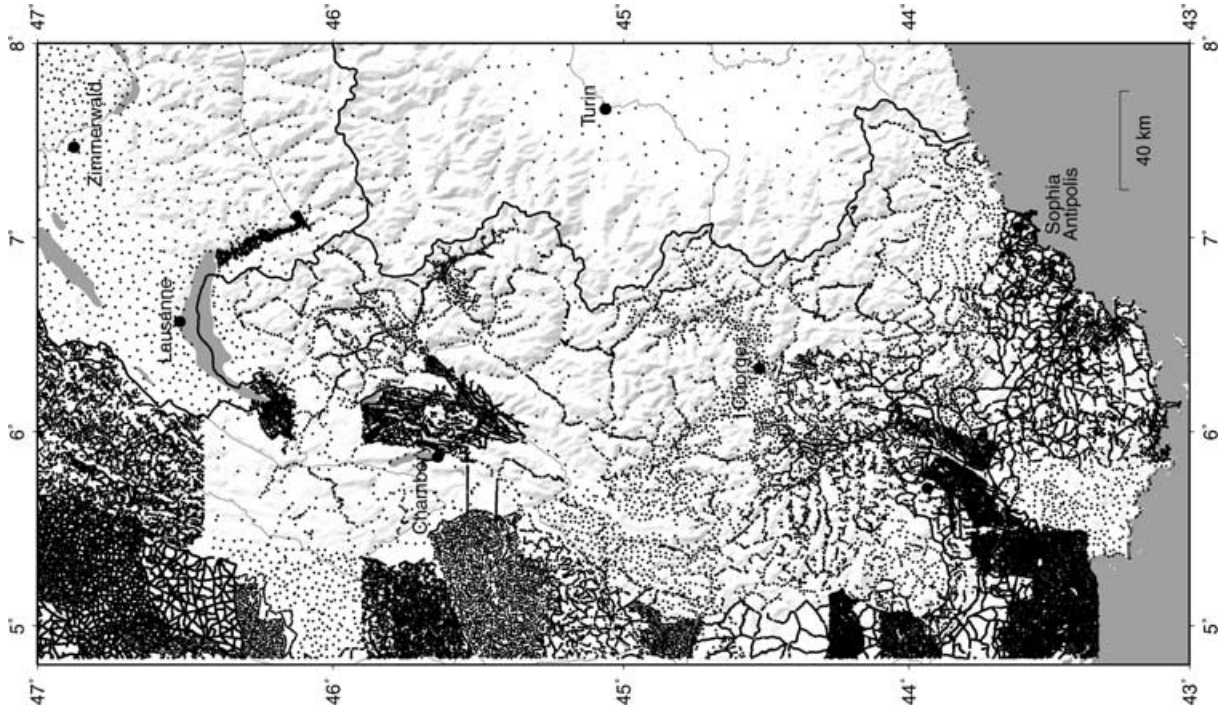

Figure 5. Locations of all the available surface gravity stations obtained from recent gravity surveys (GéoFrance 3-D research program) and from the BGI database. Grey areas are rivers and lakes.

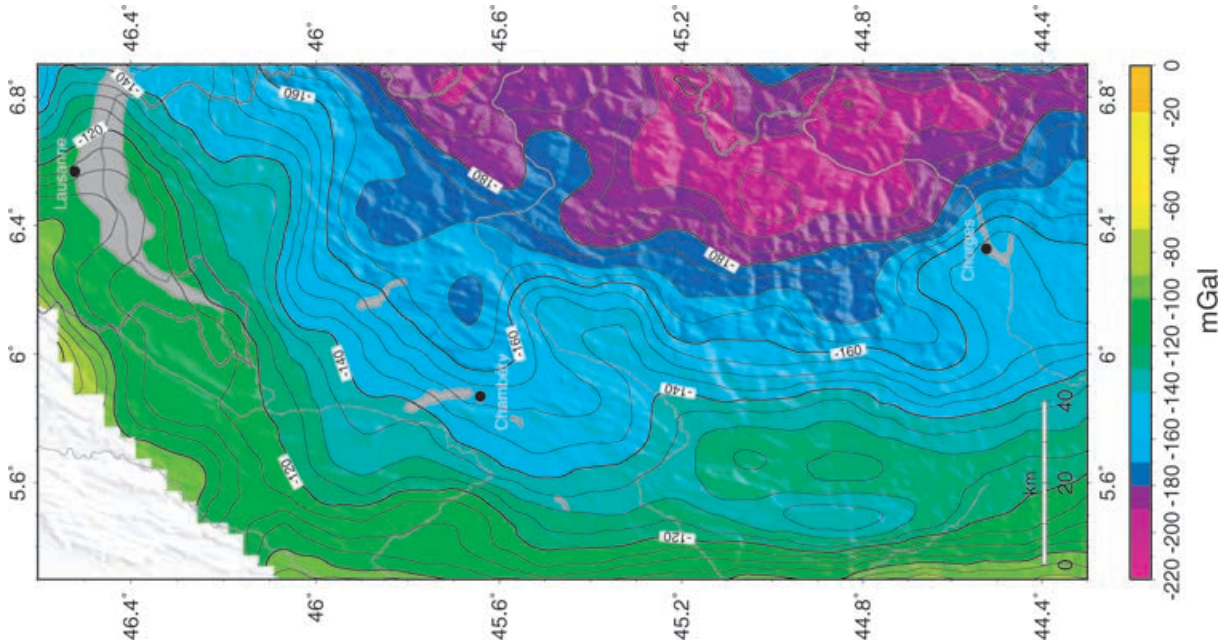

Figure 4. Complete Bouguer anomaly at 5100 m a.s.l. calculated from airborne gravity measurements; topographic corrections up to 167 km with a constant density of 2670 kg m^{-3}. Grey areas are rivers and lakes.

this database merges 76′517 gravity measurements provided by different surveys, measurements are not regularly distributed in space. This is especially true on flanks and tops of mountains which have a reduced data density compared to low land (e.g. the Rhone Valley, Fig. 5). Gridding such a data set is rather tricky since interpolation procedures are time-consuming, and more importantly the shape of the resulting contour levels is unavoidably too constrained close to the zones with dense data coverage. Such an effect was avoided by extracting from the original database a set of measurements (3′258) with a nearly constant sampling in space (Fig. 6). Because the short gravity field wavelengths ($\lambda < 5$ km) are strongly attenuated by upward continuation, a spatial sampling of a few km is sufficient for the land Bouguer gravity anomaly map intended for upward continuation.

4.2 Topographic corrections

The topographic effect was computed by numerical integration using two terrain models covering all of the Alps, and extending 200 km

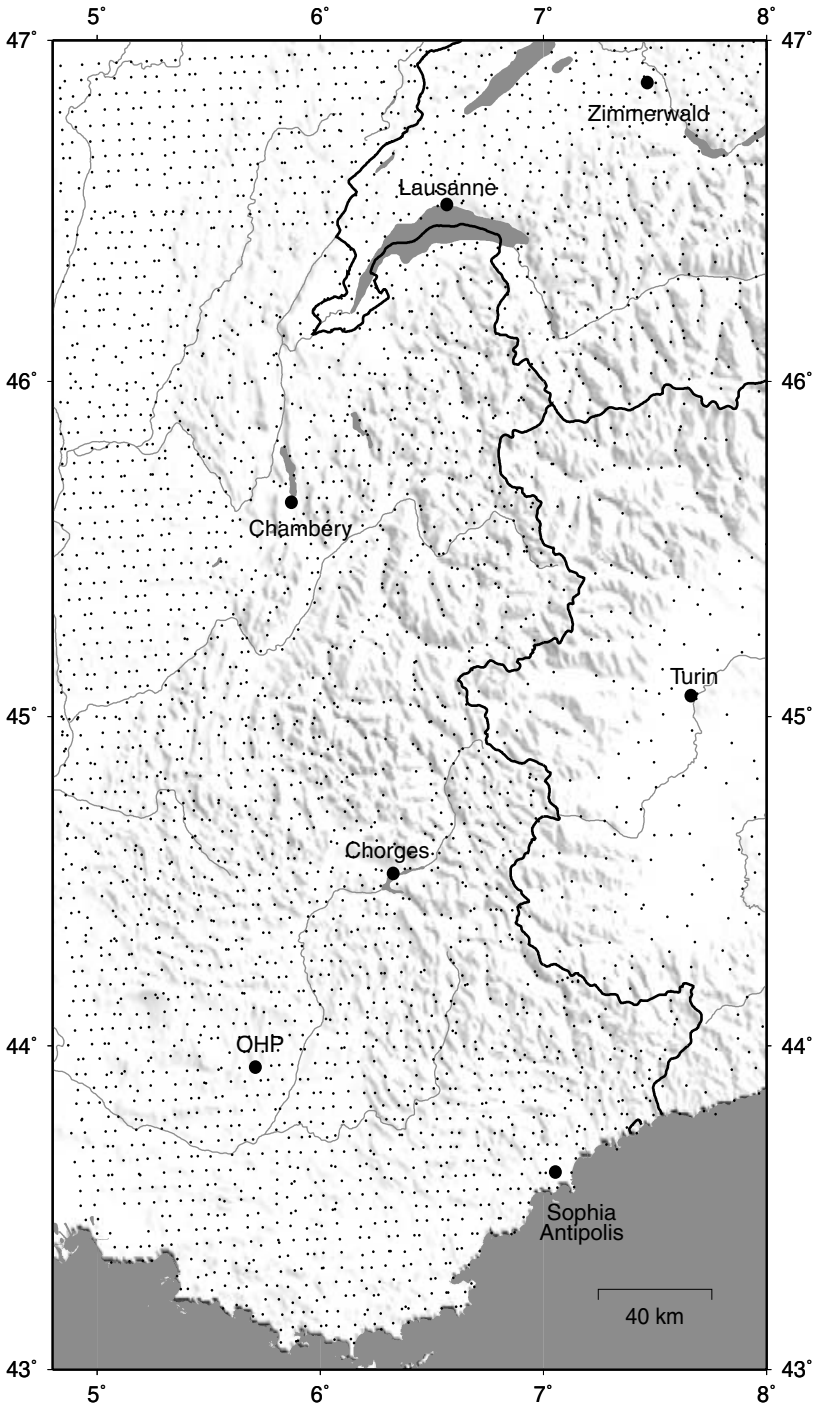

Figure 6. Locations of the stations extracted from the available database shown in Fig. 5, and used for producing the surface Bouguer gravity anomaly map of Fig. 7.

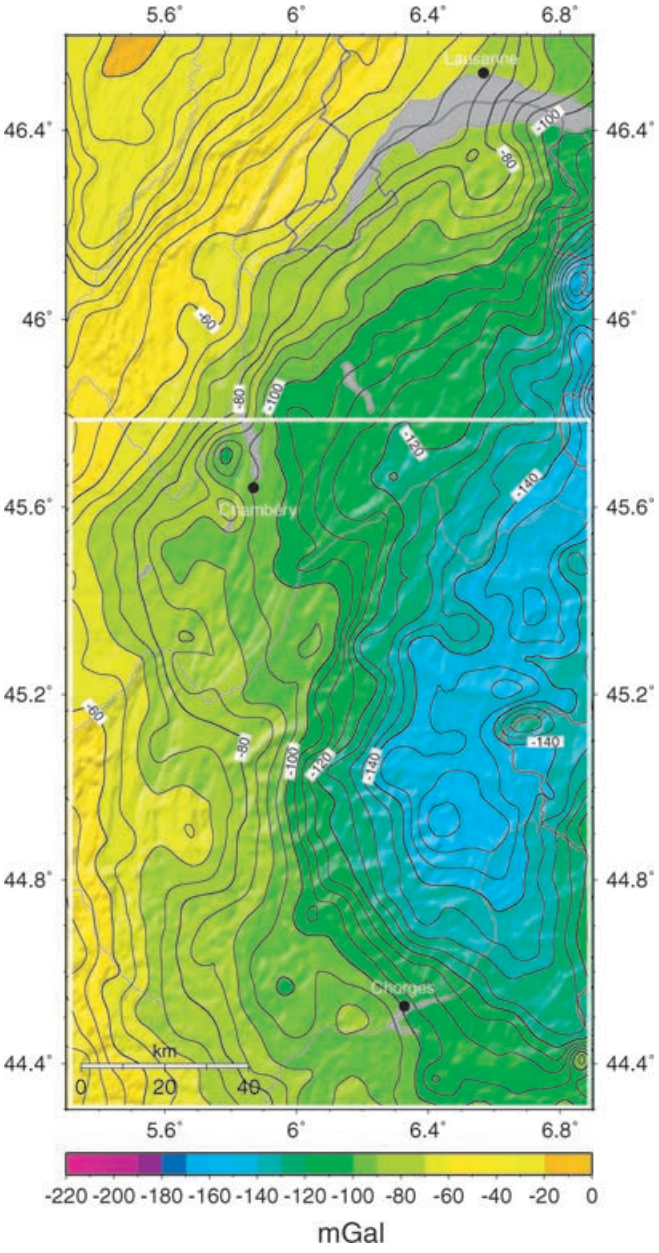

Figure 7. Bouguer anomaly map calculated from surface measurements; topographic corrections up to 167 km with a constant density of 2670 kg m^{-3}. Grey areas are rivers and lakes.

into the hinterland, with a density of correction equal to 2670 kg m^{-3} (Klingelé & Olivier 1980). The first model consists of altitude cells of 1′ by 1′ and was used for the topographic corrections around the measurement points from 10 to 26 km. For topographic corrections ranging from 26 km to 167 km, we used a second model consisting of altitude cells of 3′ by 3′. For topographic corrections closer than 10 km, we used the values provided by the BGI and Masson *et al.* (1999).

4.3 Upward continuation of the surface Bouguer gravity anomaly

Values of the Bouguer gravity anomaly derived from land measurements were gridded by means of kriging using a linear variogram (Fig. 7). The same procedure was used to grid the altitudes of the surface gravity stations, thus providing the so-called support surface. At that stage, we selected a test zone containing very different topographic features, and covered by a sufficient number of airborne measurements (Fig. 8a). The continuation of the surface Bouguer gravity anomaly was performed in two steps. The first step consisted in continuing the surface Bouguer field from the

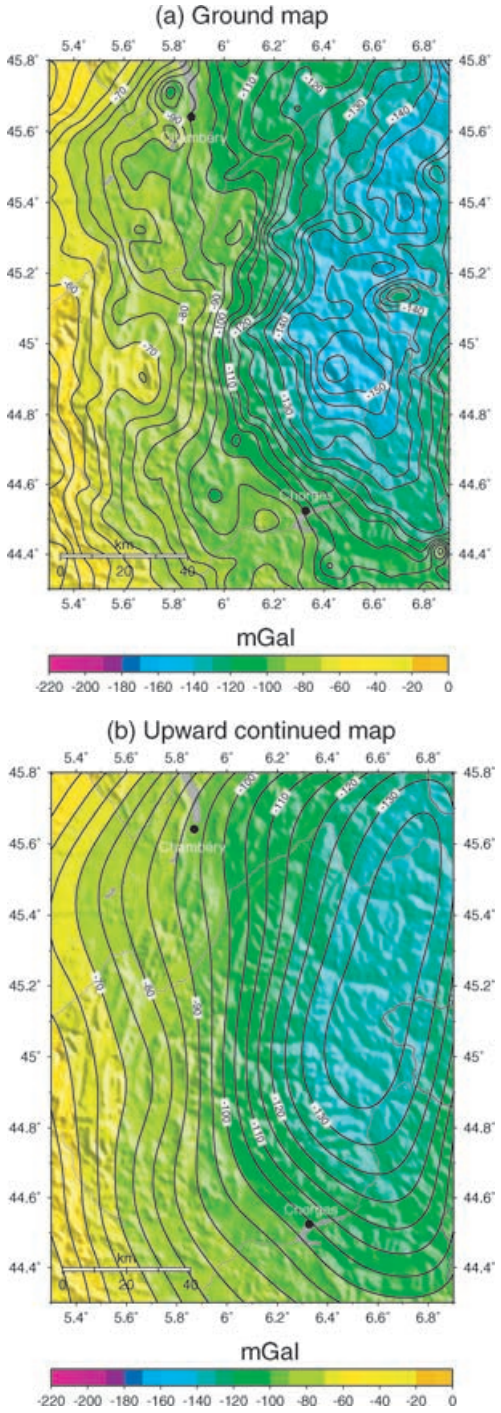

Figure 8. (a) The Bouguer anomaly map calculated from surface measurements in the subarea shown by box in Fig. 7. (b) The continuation has been performed by means of an equivalent source technique (Graber-Brunner *et al*. 1992) from the support surface to 2100 m a.s.l., and from 2100 m a.s.l. to 5100 m a.s.l. by FFT. Grey areas are rivers and lakes.

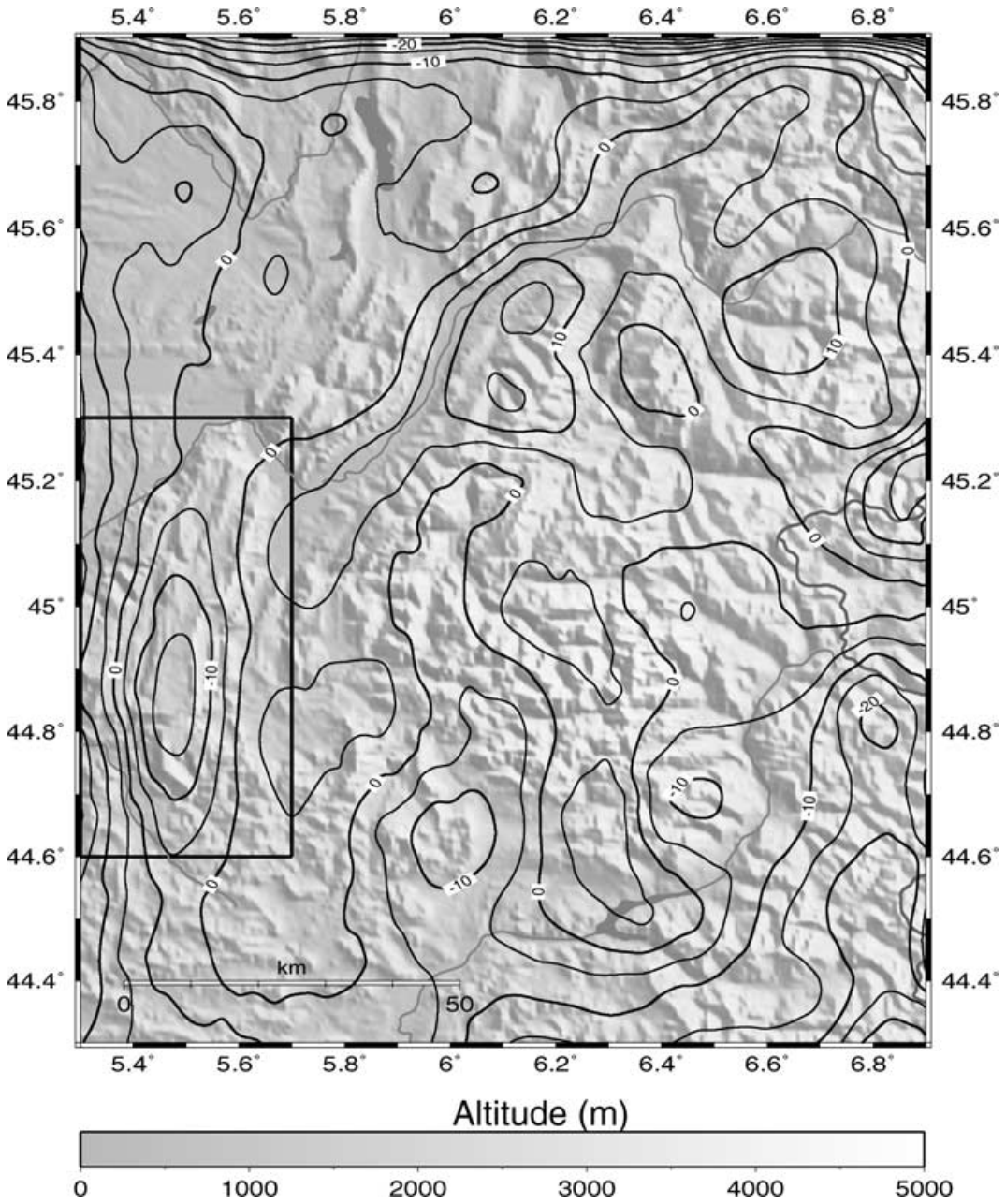

Figure 9. Contour map of the differences in mGal between the airborne Bouguer anomaly values and the upward continued surface Bouguer anomaly values superimposed on the topography (color map) in the area shown in Fig. 8. The differences in the two Bouguer fields are highly correlated to topography in the small rectangular zone marked on the left side of the figure.

irregular support surface up to a horizontal plane located above the highest surface gravity station (2100 m). For this task, we used the equivalent layer method (Graber-Brunner *et al.* 1992; Klingelé 1997). Once the Bouguer gravity anomaly had been determined on a horizontal surface, then a classical FFT-based upward continuation was used for continuing the anomaly up to the survey altitude (5100 m).

When compared to the Bouguer gravity anomaly derived from airborne data, the above-mentioned upward continued surface field has a similar shape and amplitude range. However there is a constant shift between the two fields. This can be readily explained by looking at the upward continuation operator, given in the wave domain by

$$G(u, v, z) = G(u, v, 0)\, e^{-\frac{2\pi}{\lambda} z}, \tag{4.1}$$

where G represents the 2-D Fourier transform of the Bouguer anomaly, $\lambda = \frac{1}{\sqrt{u^2 + v^2}}$ the wavelength of the anomaly, and z the vertical distance between the two planes.

It is clear that the exponential term $e^{-\frac{2\pi}{\lambda} z}$ acts as a damping factor (amplifier for downward continuation) which tends to 0 for wavelengths tending to 0 (short wavelengths). Consequently wavelengths which are long in comparison to z are left unattenuated and will be present in the airborne measurements. If the zone of the surface data considered is too small, then the long wavelength constituents present in the airborne data will be lost in the windowing process

used as part of the FFT-based upward continuation. The lost long wavelength constituents can be reasonably approximated as a constant shift, and therefore a shift of −55 mGal was applied to all values of the upward continued Bouguer gravity anomaly (Fig. 8b).

4.4 Differences between airborne and upward continued surface Bouguer gravity anomalies

Fig. 9 shows a map of the differences between the airborne acquired Bouguer gravity anomaly values and the upward continued surface Bouguer gravity anomaly values over the survey area. Over most of the survey zones of dense surface gravity data coverage, amplitudes in the field of differences range from −5 mGal to +5 mGal, thus engendering confidence in the accuracy of the airborne measurements. However, the differences can reach greater amplitudes (up to 10 mGal) in zones containing rugged topography, leading to a resulting rms difference between the two Bouguer fields of 7.68 mGal. In these zones, differences are highly correlated with the topographic relief. This effect presumably results from the use of an incorrect density value in the computation of the topographic corrections to the ground gravity data. To test this assumption, we examined the effect of modifying the density used in the topographic corrections by a factor of 10 per cent ($\Delta\rho = 300$ kg m^{-3}) on the value of the differences calculated over a small mountainous area (Fig. 10). From the comparison of the differences before and after this transformation, it is clear that the difference values are substantially reduced by up to 10 mGal, especially for the anomalies located above the highest mountains. This demonstrates conclusively the significance of using a correction density as close as possible to the true value of the rock. This task is rather tricky particularly in areas with rugged topography where the density contrasts of the rock can change significantly over small distances.

When carrying out land gravity surveys in mountainous areas, the measurement points are mostly located in the valleys and on the flanks of the mountains, rarely on the peaks. As a consequence, the gravity field at these points is affected by masses situated both below and above the measurement position. The contribution of the lower and the upper masses to the gravitational effect of the topography at the measurement point have opposite signs. When calculating along the vertical pointing downwards, the contribution of masses located below the gravity stations is positive, and negative for the masses located above. As mentioned before (*cf.* Section 4.3, eq. 4.1), the continuation operator acts in the wave domain as a damping factor which never crosses the zero axis, and therefore cannot transform a negative contribution to a positive one. As a result, when performing upward continuation, all the gravitational contributions of the topographic masses located above the points of the support surface are eliminated, and by so doing, the resulting values at survey altitude are smaller than the actual values, which contain the contribution of all the topographic sources with a positive sign. This undesirable effect increases the gap between upward continued and airborne acquired Bouguer gravity anomalies

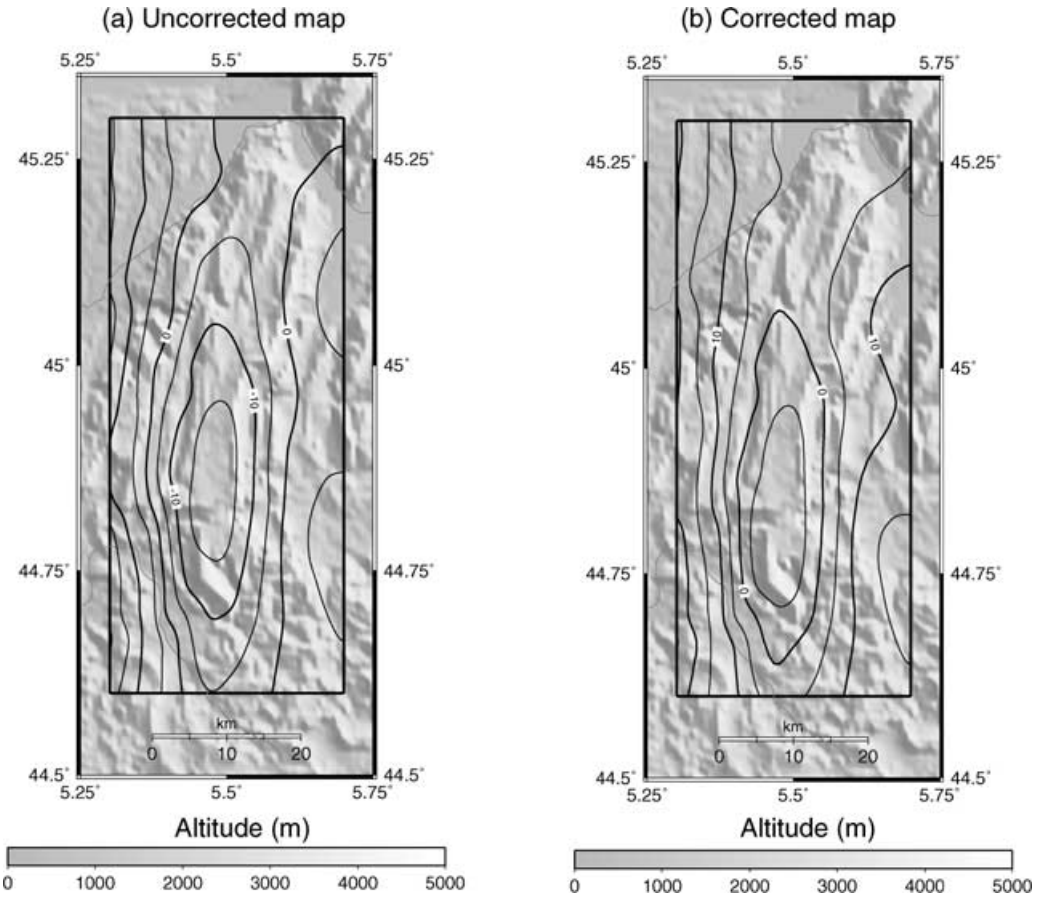

Figure 10. (a) Enlarged difference map in the subarea shown by box in Fig. 9. (b) Same difference map as shown in Fig. 10(a) corrected for an inaccurate density used in the topographic corrections. The density of rock has been increased by $\Delta\rho = 300$ kg m^{-3}. The difference values have been substantially reduced by up to 10 mGal, especially for the anomalies located above the highest mountains.

in regions containing rugged topography. Our results suggest that whichever method is used to perform upward continuation, the resulting Bouguer gravity anomaly is not entirely comparable to the airborne acquired Bouguer gravity anomaly, particularly in mountainous areas where the density distribution may not be sufficiently well known to compute accurate terrain corrections, and the upward continued values of the Bouguer gravity anomaly are unavoidably underestimated.

Through the application of low-pass filtering necessary to remove motion effects as well as attenuation due to distance from the gravity source, airborne data does not resolve short wavelength features in gravity field. However, over mountainous regions, short wavelengths in the gravity field measured at the surface are often contaminated by inaccurately calculated terrain corrections, the effects of which are attenuated in airborne data measured at high altitude above the topography. In addition, airborne data has advantages over land data, especially in mountainous areas: it is evenly sampled and the reduction from free-air to Bouguer corrected fields is much easier.

4.5 Conclusions

The results obtained are another example of why airborne gravimetry is a very promising method, especially for large scale and low sensitivity gravity surveys in mountainous terrain. The resolution and the precision of the airborne Bouguer anomaly map of the Western Alps are comparable to those of the surface Bouguer anomaly map in the same region: the rms difference between the two Bouguer fields calculated at all gridpoints without any density correction is equal to 7.6 mGal for wavelengths greater than 16 km. Moreover, airborne gravity surveying is significantly faster than terrestrial surveying (by a factor ranged from 1 to 500), and in the case of the Alps, for a cost equal or even smaller.

Airborne gravity measurements differ from land gravity measurements in that the gravity field can be regularly sampled on a horizontal surface. Thereby, some gravity field wavelengths originated from interesting geological structures, which are likely to be spatially aliased in unevenly distributed land data, can be better recovered using airborne data. Technically speaking, all the 2-D field transformations can be directly performed without any restriction in the wave domain using airborne data located on a horizontal plane, thus engendering confidence in the resulting gravity maps. Because gravity data are measured at high altitudes above the topography, the effects of inaccurately calculated terrain corrections are significantly attenuated.

ACKNOWLEDGMENTS

This work has been sponsored by a French research programme 'GéoFrance 3-D' initiated by the CNRS, the BRGM, the ministries of Industry, Research and Public Education. We are indebted to E. Calais (UMR CNRS Géosciences Azur, France) and F. Jouanne (Université de Savoie, France) for their technical help, and also to all volunteers who supervised the GPS stations. The full support of the 'Bundesamt für Militärflugplätze' (BAMF) was essential in insuring the success of the project. We are especially grateful to Mr R. Hübscher, Mr Baumberger, Mr M. Escher and Mr G. Gugger for their help throughout the project. Two of us (J. V. and R. B.) wish also to express our special thanks to Prof. Dr H.-G. Kahle of the Geodesy and Geodynamic Laboratory of the ETH Zurich, and to all of its members for their kindness and technical assistance.

REFERENCES

Balmino, G., Sabadini, R., Tscherning, C. & Woodworth, P., 1996. Modern concepts, concerns and satellite projects in the determination and use of the Earth's gravity field, *ESA N-SP-1196,* ESA Publications.

Bell, R., Coakley, B. & Stemp, R., 1991. Airborne gravimetry from a small twin engine aircraft over the Long Island Sound, *Geophysics,* **56,** 1486–1493.

Bell, R., Coakley, B., Blankenship, D., Hodge, S., Brozena, J. & Jarvis, J., 1992. Airborne gravity from a light aircraft: CASERTZ 1990–1991, in *Recent Progress in Antartic Earth Sciences,* pp. 571–577, eds Yosidha, Y., *et al.* Terra Scientific Publishing Company, Tokyo.

Bell, R., Childers, V., Arko, R., Blankenship, D. & Brozena, J., 1999. Airborne gravity and precise positioning for geologic applications, *J. geophys. Res.,* **104,** 15 281–15 292.

Blakely, R., 1996. *Potential Theory in Gravity and Magnetic Applications,* Cambridge University Press, Cambridge.

Brozena, J., 1984. A preliminary analysis of the NRL airborne gravimetry system, *Geophysics,* **49,** 1060–1069.

Brozena, J., 1994. CASERTZ 91–92: Kinematic GPS, airborne gravity and surface topography (abstract), *EOS, Trans. Am. geophys. Un.,* **75,** 102.

Brozena, J. & Peters, M., 1988. An airborne gravity study of eastern north Carolina, *Geophysics,* **53,** 245–253.

Brozena, J., Chalona, M., Forsberg, R. & Mader, G., 1992. The Greenland aerogeophysics project (abstract), *EOS, Trans. Am. geophys. Un.,* **73,** 130.

Childers, V., Bell, R. & Brozena, J., 1999. Airborne gravimetry: an investigation of filtering, *Geophysics,* **64,** 61–69.

Cocard, M., 1995. High precision GPS processing in kinematics mode, Nr 10874, 140 pages, *PhD thesis,* Swiss Fedral Institute of Technology, Zürich.

Duquenne, H., 1997. Le modèle du quasi-géoide français QGF 96 et la surface de référence d'altitude RAF96, *IGN/LAREG et ESGT, rapport interne*.

Graber-Brunner, V., Klingelé, E. & Marson, I., 1992. An improved solution for the problem of upwad continuation of gravity field data in rugged topography, *Boll. Geof. Teor. Appl.,* **23,** 135–144.

Gumert, W., 1995. Third generation aerogravity system, *Internat. Symp. on Kinematic Systems in Geodesy, Geomatics and Navigation,* pp. 153–162. University of Calgary, Canada.

Halliday, M., 1997. *LaCoste & Romberg Air-Sea Gravity Meter and 'SEASYS' Digital Control System, Instruction Manual,* LaCoste and Romberg Gravity Meters Inc., Austin.

Harlan, R., 1968. Eötvös corrections for airborne gravimetry, *J. geophys. Res.,* **73,** 4675–4679.

Klingelé, E., 1997. 2-D gravimetric study of the crystalline basement of the Rawyl depression, in *Deep structure of the Swiss Alps, results of NRP 20,* pp. 154–159, ed. O.E. Pfiffner, Birkhaüser Verlag, Basel.

Klingelé, E. & Olivier, R., 1980. La nouvelle carte gravimétrique de la Suisse, *Matériaux pour la Géologie de la Suisse, Série Géophysique 31,* Swiss Commission of Geophysics, Bern.

Klingelé, E., Cocard, M., Halliday, M. & Kahle, H.-G., 1996. The airborne gravimetric survey of Switzerland, *Contribution to the Geology of Switzerland—Geophysical Series,* **31,** 104. *31,* Swiss Commission of Geophysics, Bern.

Klingelé, E., Cocard, M. & Kahle, H.-G., 1997. Kinematic GPS as a source for airborne gravity reduction in the airborne gravity survey of Switzerland, *J. geophys. Res.,* **102,** 7705–7715.

LaCoste, L., 1967. Measurements of gravity at sea and in the air, *Geophysics,* **5,** 477–526.

LaCoste, L., Ford, J., Bowles, R. & Archer, K., 1982. Gravity measurements in an airplane using state-of-the-art navigation and altimetry, *Geophysics,* **47,** 832–838.

Masson, F., Verdun, J., Bayer, R. & Debeglia, N., 1999. Une nouvelle carte gravimétrique des Alpes Occidentales et ses conséquences structurales et tectoniques, *C. R. Acad. Sci. Paris,* **329,** 865–871.

Mittal, P., 1984. Algorithm for error adjustment of potentiel-field data along a survey network, *Geophysics,* **49,** 467–469.

Moritz, H., 1988. Geodetic reference system 1980, *Bulletin Géodésique, The Geodetists Handbook, International Union of Geodesy and Geophysics,* IAG Publications, France.

Olesen, A. & Forsberg, R., 1995. Airborne gravimetry using LaCoste and Romberg gravimeter-An error analysis, *Internat. Symp. on Kinematic Systems in Geodesy, Geomatics, and Navigation,* pp. 613–617, University of Calgary, Canada.

Post, E. J., 1967. Sagnac effect, *Rev. Mod. Phys.,* **19,** 475.

Rothacher, M. & Mervart, L., 1996. *Bernese GPS software version 4.0,* Astronomical Insitute of the University of Berne, Berne.

Thompson, L. & LaCoste, L., 1960. Aerial gravity measurements, *J. geophys. Res.,* **65,** 305–322.

Verdun, J., Bayer, R., Klingelé, E., Cocard, M., Geiger, A. & Halliday, M., 2002. Airborne gravity measurements over mountainous areas by using a LaCoste and Romberg air-sea gravity meter, *Geophysics,* **67,** 807–816.

Wessel, P., 1989. XOVER. A crossover error detector for track data, *Comput. Geosci.,* **15,** 333–346.